The Plant Cell, Vol. 8, 2155–2168, December 1996 © 1996 American Society of Plant Physiologists

RESEARCH ARTICLE

Identification of a Meristem L1 Layer-Specific Gene in Arabidopsis That Is Expressed during Embryonic Pattern Formation and Defines a New Class of Homeobox Genes

Pengzhe Lu,[1] Ron Porat,[1] Jeanette A. Nadeau,[2] and Sharman D. O'Neill[3]

Section of Plant Biology, Division of Biological Sciences, University of California at Davis, Davis, California 95616

Homeobox genes are master regulatory genes that specify the body plan and control development of many eukaryotic organisms, including plants. We isolated and characterized a cDNA designated *ATML1* (for *Arabidopsis thaliana* meristem L1 layer) that encodes a novel homeodomain protein. The ATML1 protein shares high sequence homology inside and outside of the homeodomain with both the Phalaenopsis O39 and the Arabidopsis GLABRA2 (GL2) homeodomain proteins, which together define a new class of plant homeodomain-containing proteins, designated HD-GL2. The *ATML1* gene was first expressed in the apical cell after the first asymmetric division of the zygote and continued to be expressed in all proembryo cells until the eight-cell stage. In the 16-cell proembryo, the *ATML1* gene showed a distinct pattern of expression, with its mRNA becoming restricted to the protoderm. In the torpedo stage of embryo development, *ATML1* mRNA disappeared altogether but reappeared later only in the L1 layer of the shoot apical meristem in the mature embryo. After germination, this L1 layer-specific pattern of expression was maintained in the vegetative shoot apical meristem, inflorescence, and floral meristems, as well as in the young floral organ primordia. Finally, *ATML1* mRNA accumulated in the protoderm of the ovule primordia and integuments and gradually became restricted in its expression to the endothelium surrounding the embryo sac. We propose that *ATML1* may be involved in setting up morphogenetic boundaries of positional information necessary for controlling cell specification and pattern formation. In addition, *ATML1* provides an early molecular marker for the establishment of both apical-basal and radial patterns during plant embryogenesis.

INTRODUCTION

Although most plant development occurs after embryogenesis, the basic shoot–root body plan and the three primary tissue systems are generated during embryogenesis (Goldberg et al., 1994; Jurgens et al., 1994; Jurgens, 1995). In flowering plants, the basic organization of the plant body can be described as a superimposition of two patterns: one along the apical–basal axis of polarity and the other following a radial pattern perpendicular to the axis (Goldberg et al., 1994; Jurgens et al., 1994; Jurgens, 1995). In Arabidopsis, the apical–basal pattern appears to be established with the first asymmetric division of the zygote that gives rise to a small upper terminal cell and a large lower basal cell. The small terminal cell will develop into the embryo proper and will form most of the mature embryo, including the shoot meristem, cotyledons, hypocotyl, and part of the embryonic root. The large basal cell will form the suspensor and root meristem (West and Harada, 1993; Goldberg et al., 1994; Jurgens, 1995). Radial pattern formation starts at the 16-cell proembryo stage coincident with periclinal divisions that result in the formation of an outer cell layer, the protoderm, which is the precursor of the epidermis. Subsequent cell differentiation within the inner cell mass results in the production of a middle layer of ground meristem tissue and an inner procambium layer that will form the vascular tissue (West and Harada, 1993; Goldberg et al., 1994; Jurgens et al., 1994; Jurgens, 1995).

After seed germination, the shoot and root apical meristems retain some properties of embryonic cells and become active to produce the postembryonic shoot and root systems of the adult plant (Sussex, 1989). Early observations suggested that the shoot apical meristem is divided into two regions: the tunica and the corpus. Whereas the cells of the tunica divide

[1] These authors contributed equally to the experimental work presented in this study.

[2] Current address: Department of Plant Biology, Ohio State University, 1735 Neil Avenue, Columbus, OH 43210-1293.

[3] To whom correspondence should be addressed.

anticlinally and increase the apex surface, the cells of the corpus have irregular planes of divisions and increase the apex volume (Schmidt, 1924). Later, it was suggested that in most dicotyledonous plants, the shoot apical meristem consists of three superimposed cell layers: a superficial L1, a subsurface L2, and a deeper L3 layer (Satina et al., 1940). The epidermis was found to be generated exclusively by the L1 layer of the meristem. In Arabidopsis, the shoot apical meristem consists of two tunica layers (equivalent to L1 and L2) overlying a shallow corpus (Barton and Poethig, 1993).

The establishment of the apical–basal and radial spatial patterns of development during embryogenesis and their maintenance in the apical meristem have been the focus of many studies (West and Harada, 1993; Goldberg et al., 1994; Jurgens et al., 1994; Jurgens, 1995; Meinke, 1995). Recent advances in studies of animal embryogenesis have provided clues to the mechanisms by which genes control patterning (Gurdon, 1992; Lawrence and Morata, 1994). Families of homeobox genes in both the animal and plant kingdoms have been found to play important roles in developmental decisions that control cell specification and pattern formation (Gehring et al., 1994; Lawrence and Morata, 1994). The homeobox genes share a common sequence element of 180 bp, the homeobox, that encodes the 60–amino acid homeodomain, which represents the DNA binding domain (Laughon, 1991; Kornberg, 1993).

Different homeobox genes have been grouped into specific families or classes based on either sequence identity within the homeodomain or conserved protein motifs outside of the homeodomain (Gehring et al., 1994). In plants, four different types of homeodomain proteins have been described (Kerstetter et al., 1994): homeodomain zipper proteins that are distinguished by the presence of a leucine zipper adjacent to the homeodomain (Ruberti et al., 1991; Mattson et al., 1992; Schena and Davis, 1992, 1994), plant homeodomain finger proteins that share a conserved cysteine-rich motif (Bellmann and Werr, 1992; Schindler et al., 1993; Korfhage et al., 1994), the Arabidopsis homeodomain protein GLABRA2 (GL2) (Rerie et al., 1994), and KNOTTED1 (KN1) and related proteins (Volbrecht et al., 1991; Lincoln et al., 1994; Ma et al., 1994). In addition, two more Arabidopsis homeodomain proteins that share high sequence similarity between themselves have been identified recently (Quaedvlieg et al., 1995; Reiser et al., 1995).

There are several animal homeobox genes that are expressed in specific germ layers during gastrulation and are required for specification of these cell layers (reviewed in Boncinelli and Mallamaci, 1995). Examples include the mouse *goosecoid* and *Lin1*, which are expressed in the anterior mesoderm (Blum et al., 1992; Shawlot and Behringer, 1995), and *Otx2*, which is expressed in the anterior ectoderm (Ang et al., 1994). Both the *goosecoid* and *Lin1* genes were found to be involved in the formation of the anterior head structures, and *Otx2* was suggested to be involved in the anterior specification of the central nervous system. By analogy, it is likely that plant homeobox genes play similar roles in specifying the identity of specific cell layers or tissues.

There are several plant homeobox genes that have been proposed to be involved in defining morphogenetic boundaries of positional information and determining cell fate in both the embryo and the shoot apical meristem. It is likely that groups of these homeodomain proteins interact to determine organization of the embryo and apical meristems. The *KN1* gene in maize and *SHOOT MERISTEMLESS* (*STM*), a *KN1*-like gene in Arabidopsis, mark a specific pattern of expression coincident with shoot meristem formation in the embryo (Smith et al., 1995; Long et al., 1996). Furthermore, plants with recessive mutations at the *STM* locus fail to develop a shoot apical meristem during embryogenesis (Long et al., 1996). In the maize shoot apical meristem, *KN1* mRNA is expressed in the corpus but not in the L1 layer and was proposed to be involved in establishing the boundary of the meristem, keeping it in an undetermined state (Sinha et al., 1993; Jackson et al., 1994). *GL2* is an Arabidopsis homeobox gene required for normal trichome development. It is expressed specifically in trichome progenitor cells and is involved in determination and commitment to trichome differentiation (Rerie et al., 1994). Another Arabidopsis homeobox gene, *BELL1* (*BEL1*), is expressed in the middle region of the ovule primordium and interprets positional information to control morphogenesis of the integuments (Reiser et al., 1995). In Phalaenopsis, the *O39* homeobox gene is expressed early in the differentiation of ovule primordia and was suggested to be involved in the commitment to ovule development (Nadeau et al., 1996).

In this study, we describe the identification and characterization of a novel Arabidopsis homeobox gene, *ATML1* (for *Arabidopsis thaliana* meristem L1 layer), which is expressed specifically in the L1 layer of the meristem from the very earliest stages of meristem patterning and throughout shoot development. In addition, the differential expression of *ATML1* in defined cells of the early proembryo suggests a regulatory role for this gene in apical–basal and radial pattern formation. The ATML1 homeodomain-containing protein shares considerable sequence similarity with two other homeodomain proteins, Arabidopsis GL2 and Phalaenopsis O39 (Rerie et al., 1994; Nadeau et al., 1996), and together these three genes define a new family of homeobox genes in higher plants.

RESULTS

Molecular Cloning of the *ATML1* cDNA

In a previous study, we isolated several ovule-specific cDNAs from orchid flowers, including a homeobox gene designated *O39* (Nadeau et al., 1996). In this work, we screened an Arabidopsis floral bud cDNA library with *O39* as a probe and isolated its Arabidopsis homolog named *ATML1*. The full-length cDNA sequence of *ATML1* consists of 2940 bp, with an open reading frame of 2154 bp. The *ATML1* gene encodes a protein of 718 amino acids, with a predicted molecular mass of ~73 kD and a pI of 5.74. *ATML1* contains a homeodomain DNA bind-

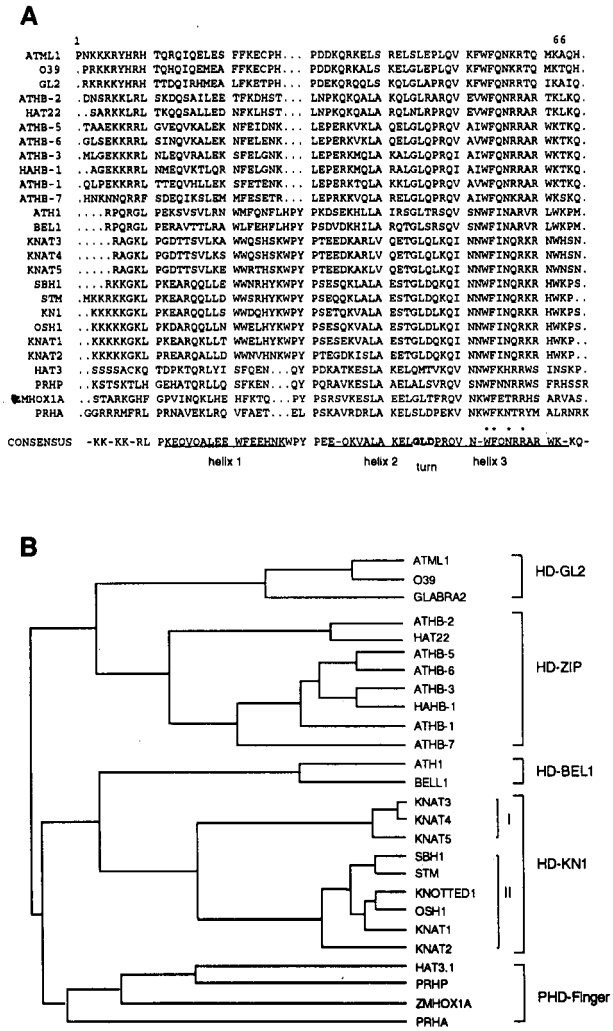

Figure 1. Amino Acid Sequence Alignment and Phylogenetic Comparison of the ATML1 Homeodomain with Other Plant Homeodomains.

(A) Amino acid sequence alignment of the ATML1 homeodomain with other homeodomains representing the major classes of plant homeobox genes. The most invariant residues in helix 3 are indicated by asterisks. The GenBank accession numbers corresponding to the various plant sequences are as follows: *ATML1*, U37589; *O39*, U34743; *GL2*, L32873; *ATHB-2*, X68145; *HAT22*, U09337; *ATHB-5*, X67033; *ATHB-6*, X67034; *ATHB-3*, X62644; *HAHB-1*, L22847; *ATHB-1*, X58821; *ATHB-7*, X67032; *ATH1*, X80126; *BEL1*, U39944; *KNAT3*, X92392; *KNAT4*, X92393; *KNAT5*, X92394; *SBH1*, L13663; *STM*, U32344; *KN1*, U14174; *OSH1*, D16507; *KNAT1*, U14174; *KNAT2*, U14174; *HAT3*, X69512; *PRHP*, L21975; *ZmHox1A*, X67561; *PRHA*, L21991.

(B) Phylogenetic analysis of amino acid similarity of the various plant homeodomains presented in **(A)**. The homeodomain leucine zipper proteins were named HD-ZIP, and the plant homeodomain finger proteins were named PHD-Finger.

ing motif within its N-terminal region between amino acid residues 17 to 78 (Figures 1A and 2B). The *ATML1* homeodomain contains all of the four highly conserved amino acid residues of the third recognition helix that serve as a signature for homeodomain proteins as well as four out of six additional amino acids at other conserved positions within the homeodomain (Figure 1A; Laughon, 1991).

ATML1 Is a Member of a New Class of Higher Plant Homeobox Genes

By comparing the *ATML1* homeodomain with other representatives of the major classes of plant homeodomains (Kerstetter et al., 1994), we found that the ATML1 homeodomain shares 94% similarity with O39 and 79% with GL2 but has much less sequence similarity to other plant homeodomains. For example, the ATML1 homeodomain shares only 37% similarity with either the KN1 or BEL1 homeodomains (Figure 1A). The phylogenetic comparison shown in Figure 1B illustrates the degree of similarity to other plant homeodomains and defines ATML1 together with O39 and GL2 as a new class of plant homeodomain proteins. Because *GL2* was the first gene isolated among these three (Rerie et al., 1994), we named the class HD-GL2 (for homeodomain GL2).

All three members of the HD-GL2 class of homeobox genes share some overall similarities that significantly distinguish them from other homeobox genes. Within the homeodomain, the identity among ATML1, O39, and GL2 is dispersed along the entire region and is especially conserved in the third recognition helix, in which the proteins share 13 of 16 identical amino acids (Figures 1A and 2B). At the N-terminal arm of the homeodomain, all of the HD-GL2 proteins share a conserved basic end, in which the basic amino acids His, Lys, and Arg consist of seven of the last nine residues (Figures 1A and 2B). In addition, the HD-GL2 proteins share a conserved deletion of three amino acids between helices 1 and 2 (Figure 1A). At the N-terminal region, outside of the homeodomain proper, the HD-GL2 proteins share an acidic domain enriched with the amino acid residues Asp and Glu (Figure 2B). At the C-terminal region, contiguous with the homeodomain, all of the HD-GL2 proteins share two conserved hydrophilic regions of six and nine amino acids, followed by an uncharged polar region of 10 to 12 amino acids (Figure 2B). The conserved sequence motifs that characterize HD-GL2 proteins, within and adjacent to the homeodomain region, are further illustrated in Figure 2A.

The alignment of the predicted proteins of O39, ATML1, and GL2 shows that the amino acid identity between these proteins is dispersed along a large region of the protein, including regions outside of the homeodomain (Figure 2B). A distinctive feature of these proteins is their larger size, relative to other homeodomain proteins, of 768, 718, and 745 amino acids for O39, ATML1, and GL2, respectively (Figure 2B). Another unique characteristic of the HD-GL2 class is that the homeodomain is located at the N terminus of the protein, in contrast to most other plant and animal homeobox genes in which the

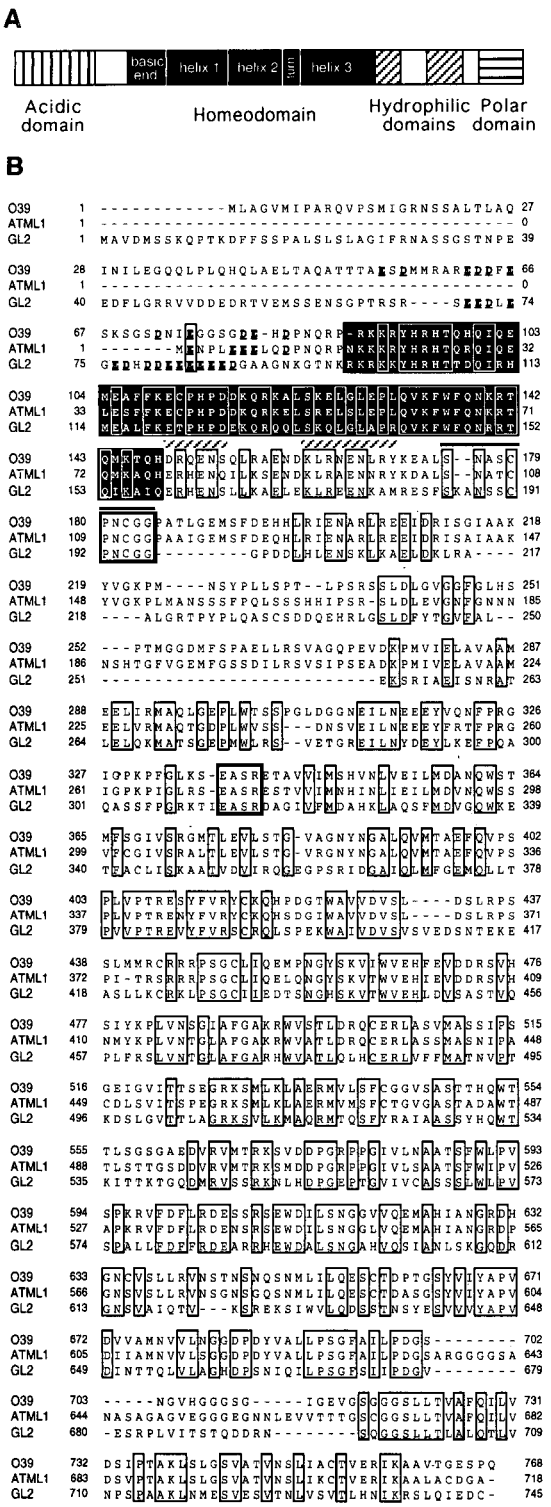

Figure 2. Comparison of Arabidopsis ATML1, Phalaenopsis O39, and Arabidopsis GL2 Proteins.

homeodomain is located near the C terminus (Figure 2B; Gehring et al., 1994). GL2 is distinctive from ATML1 and O39 by having a large gap of 28 amino acids after amino acid residue 250 (Figure 2B).

Arabidopsis HD-GL2 Proteins Are Encoded by a Small Gene Family

To determine the possible presence of other gene members of the HD-GL2 class in Arabidopsis, we performed DNA gel blot analyses using several gene-specific probes under low- and high-stringency hybridization conditions (Figures 3A and 3B). The complete cDNA of *ATML1*, including the homeobox, hybridized under low-stringency conditions with 10 to 20 different sequences in the Arabidopsis genome that probably represent different homeobox genes (Figure 3B, blot 1). However, under the same hybridization conditions, an *ATML1* 3′ end–specific probe that does not contain the homeobox hybridized with only two genomic restriction fragments (Figure 3B, blot 2). Under high-stringency conditions, using either an *ATML1* 3′ probe (Figure 3B, blot 3) or a probe containing the homeobox (Figure 3B, blot 4), the hybridization pattern suggested that *ATML1* is a single-copy gene in Arabidopsis. To determine whether the second genomic restriction fragment detected in Figure 3B, blot 2, corresponded to *GL2* or to another member of the HD-GL2 class, we reprobed the blot with a *GL2*-specific cDNA probe under similar hybridization stringency conditions. The results show that *GL2* hybridized with a unique set of Arabidopsis genomic DNA restriction fragments, indicating that the sequences are sufficiently divergent from *ATML1* that they do not cross-hybridize (Figure 3B, blot 5). Therefore, the additional genomic restriction fragments indicated by the arrowheads (Figure 3B, blot 2) probably represent an additional homeobox gene closely related to *ATML1*. Moreover, the additional 5.1-kb band that appeared after digestion with HindIII was detected by both the *ATML1* 3′-specific probe and the *ATML1* homeobox-specific probe (Figure 3B, blots 2 to 4), suggesting that this third member of the HD-GL2 gene family in Arabidospsis is related to *ATML1* both inside and outside the homeobox region.

(A) Schematic diagram illustrating the domains conserved between ATML1, O39, and GL2 proteins.

(B) Alignment of the ATML1, O39, and GL2 proteins. Those amino acids that are identical among all of the three proteins are boxed. The homeodomain region is black. The acidic amino acids upstream of the homeodomain are boldface and underlined. The hydrophilic domains contiguous with the C-terminal arm of the homeodomain region are indicated by diagonal hatching. The uncharged polar domain farther downstream of the homeodomain region is indicated by a solid line. Dashes were introduced to optimize alignment. The GenBank accession numbers of *O39*, *ATML1*, and *GL2* are U34743, U37589, and L32873, respectively.

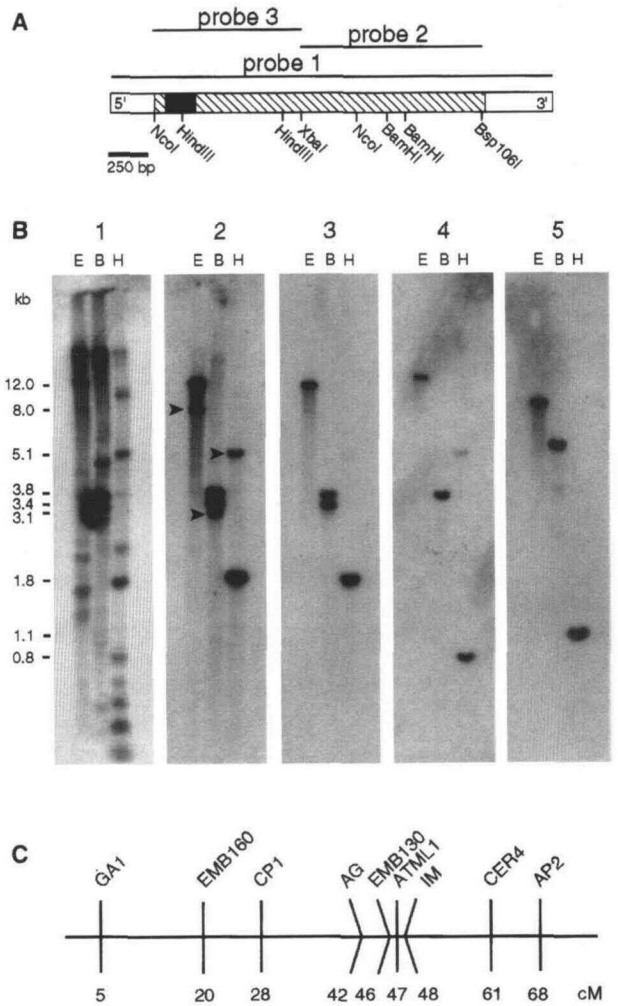

Figure 3. Genomic DNA Gel Blot Hybridization Analysis and Mapping of *ATML1*.

(A) Schematic diagram of *ATML1* cDNA showing restriction sites and the different probes used for the genomic DNA analysis shown in **(B)**.
(B) DNA gel blot hybridization analysis. Each lane contains 10 μg of genomic DNA digested with EcoRI (E), BamHI (B), or HindIII (H). The numbers at left represent the approximate lengths of the major bands detected. Genomic DNA was probed with the complete *ATML1* cDNA (probe 1) at low stringency (blot 1), an *ATML1*-specific probe (probe 2) at low (blot 2) or high (blot 3) stringency, a probe containing the *ATML1* homeobox (probe 3) at high stringency (blot 4), or a *GL2*-specific probe at high stringency (blot 5). Bands not related to either *ATML1* or *GL2* are indicated by arrowheads.
(C) The map position of *ATML1* is on chromosome 4. cM, centimorgans.

The chromosomal location of *ATML1* was determined by segregation analysis of a restriction fragment length polymorphism by using 100 recombinant inbred (RI) lines (Lister and Dean, 1993). The *ATML1* gene was mapped to chromosome 4 between the genetic markers *AGAMOUS* and m600. Following transfer to the Arabidopsis classical map, *ATML1* was located at 47 centimorgans between the *emb130* and *im* mutations (Figure 3C).

Expression of the *ATML1* Gene in Different Organs

To determine the pattern of *ATML1* mRNA accumulation in various vegetative and reproductive organs of Arabidopsis, we conducted an RNA gel blot hybridization analysis by using an *ATML1* 3′-specific cDNA probe (Figure 3A, probe 2). Figure 4 shows that a 3.0-kb transcript was detected at high levels in floral buds and at lower levels in siliques but was undetectable in roots, rosette leaf blades, and inflorescence stems of 28-day-old plants, suggesting that the *ATML1* gene is expressed only in developing shoot tissues, for example, meristems and young floral organs, but not in tissues of the root system.

In Situ Localization of *ATML1* mRNA

To define the spatial pattern of *ATML1* gene expression during different stages of plant development, we conducted RNA in situ hybridization experiments with a gene-specific *ATML1* digoxigenin-labeled antisense RNA as a probe (Figure 3A, probe 2). Figures 5A to 5L illustrate the specific accumulation of *ATML1* mRNA in different stages of embryo development. After fertilization, *ATML1* mRNA was not detected clearly in any cells within the embryo sac, including the fertilized egg (zygote) located near the micropylar end (Figure 5A). At this stage, a weak *ATML1* transcript signal was detected in the endothelial layer surrounding the embryo sac, which is likely to

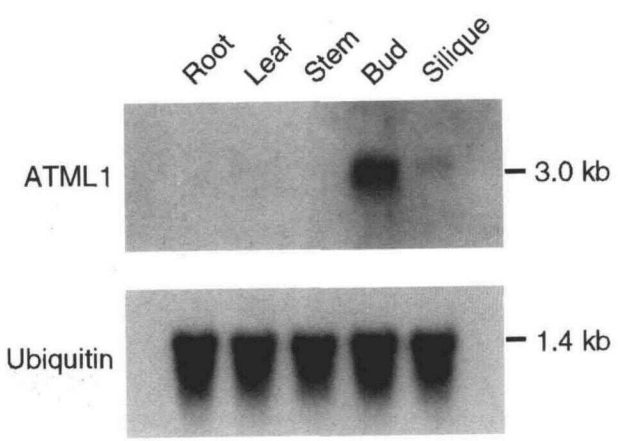

Figure 4. RNA Gel Blot Hybridization Analysis of *ATML1*.

Each lane contains 1 μg of poly(A)$^+$ RNA isolated from roots, rosette leaf blades, inflorescence stems, flower buds, or siliques from 28-day-old plants. Hybridization with a ubiquitin cDNA probe served as a control for equal loading of RNA in each lane. Numbers at right indicate the approximate lengths of the mRNAs detected.

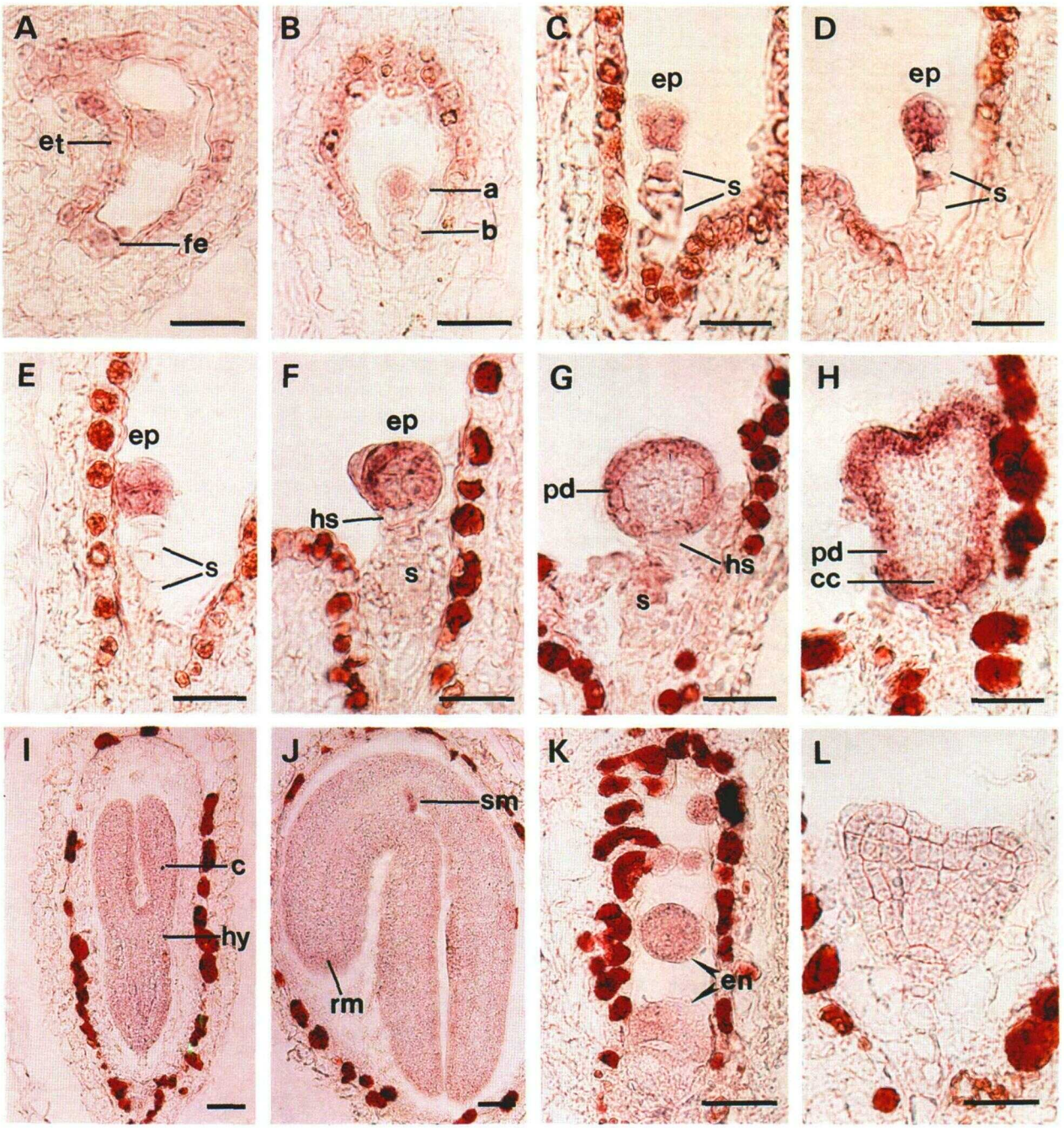

Figure 5. In Situ Localization of *ATML1* mRNA in Developing Embryos and Endosperm.

Longitudinal sections (7 μm thick) through the embryo were hybridized with either an *ATML1* antisense RNA probe (**[A]** to **[K]**) or an *ATML1* sense RNA probe as a control **(L)**. Probes were labeled with digoxigenin-UTP. The transcript-specific hybridization signal is visualized as purple color.

(A) Fertilized egg.

(B) Two-cell proembryo consisting of an apical and a basal cell.

(C) One-cell embryo proper and suspensor.

(D) Two- or four-cell embryo proper.

(E) Eight-cell embryo proper.

(F) Sixteen-cell embryo proper.

(G) Globular-stage embryo.

represent residual transcript. This observation is consistent with the fact that *ATML1* mRNA was detected at high levels in the endothelium before fertilization (Figure 6J). In addition, a brownish background color appeared in the endothelium after fertilization. This coloration represents a staining artifact, probably caused by components involved in seed coat formation (Figures 5A to 5K), because this brownish background color appeared also in control sections of developing seeds hybridized with an *ATML1* sense strand probe (Figure 5L).

After the first transverse division of the zygote, *ATML1* mRNA gradually appeared in the apical cell (terminal cell) that gives rise to the embryo proper and later forms most of the mature embryo. However, it did not appear in the basal cell that contributes to the formation of the suspensor and the hypophysis that forms the root meristem (Figure 5B). The cell-specific accumulation of *ATML1* mRNA in the apical cell became clearer after the basal cell underwent one or two transverse divisions (Figure 5C). After the apical cell divided longitudinally twice and transversely once, *ATML1* mRNA continued to be expressed uniformly in the two-, four-, and eight-cell embryo proper (Figures 5D and 5E). These results indicate that *ATML1* expression becomes restricted to the apical region of the embryo proper immediately after the first asymmetric cell division that establishes polarity of the zygote.

Differential expression of the *ATML1* gene within cells of the embryo began in the 16-cell proembryo (dermatogen embryo) in the outer layer or protoderm of eight cells, which serves as the precursor of the epidermis. *ATML1* mRNA continued to accumulate in the eight-cell protoderm but gradually declined in the inner cell mass (Figure 5F). At this stage, the hypophysis formed at the top of the suspensor and was continuous with the protoderm surrounding the inner cell mass; however, no *ATML1* mRNA was observed in the hypophysis (Figure 5F). The differential accumulation of *ATML1* mRNA in the first embryonic tissue, the protoderm, became more evident in the 32-cell embryo and was consistently observed in the globular and heart stages (Figures 5G and 5H). No *ATML1* mRNA was detected in the torpedo-stage embryo (Figure 5I), but it reappeared later in the nearly mature embryo, coincident with formation of the L1 layer of the shoot meristem (Figure 5J).

ATML1 mRNA accumulation was also detected in the developing endosperm (Figure 5K). The transcript was detected at the time of free nuclei proliferation after the endosperm had undergone several rounds of divisions, forming bubble-like structures on the periphery of the embryo sac (Figure 5K). However, compared with the specific accumulation of *ATML1* mRNA in the embryo proper and the protoderm, *ATML1* mRNA accumulation in the endosperm was weaker and without any specific patterning. No *ATML1* mRNA was detected in the endosperm at later stages of embryo development, when the free nuclei became cellularized and substantially degraded.

After seed germination, expression of *ATML1* mRNA was localized specifically in the L1 layer of the vegetative shoot apical meristem and in the protoderm of leaf primordium (Figure 6A). No *ATML1* transcript was observed in the epidermis of young and mature leaves, in the epidermis of the stem (Figure 6A), or in the root tissue including the root meristem (data not shown). After the transition from vegetative to reproductive growth, the cell-specific accumulation of *ATML1* mRNA in the L1 layer became even more pronounced, and a strong hybridization signal was observed in the single L1 layer of the inflorescence meristem (Figure 6B). Similar L1 layer–specific expression was maintained in the floral meristem (Figure 6C) and in the protoderm of floral organ primordia (Figure 6D). During later flower development, levels of *ATML1* mRNA gradually declined in the protoderm or epidermis of young floral organs, with the exception of the placenta, where ovules were later initiated (Figures 6E and 6G). After initiation of the ovule primordia, *ATML1* mRNA transiently accumulated in the outer layer of the nucellus (Figures 6F and 6H). Later, *ATML1* mRNA was also detected in the protoderm of the developing inner and outer integuments (Figure 6I). In the mature ovule, *ATML1* gene expression was detected in the endothelium, which is the inner layer of the inner integument that is in direct contact with the embryo sac (Figure 6J). Control sections hybridized with the sense strand did not show any signal (Figure 6K). Furthermore, the outer layer–specific pattern of *ATML1* expression was not due to cross-hybridization with *GL2*, because *GL2* mRNA was restricted to differentiating trichome progenitor cells of the epidermis of young leaves (Figure 6L). The L1 layer–specific pattern of *ATML1* mRNA accumulation in the shoot and flower meristems was also confirmed by RNA in situ hybridization experiments using a ^{35}S-radiolabeled probe (data not shown).

The overall pattern of *ATML1* mRNA accumulation at the different stages of embryo development and in the vegetative and reproductive organs is further illustrated in Figures 7A and 7B.

Figure 5. (continued).

(H) Heart-stage embryo.
(I) Torpedo-stage embryo.
(J) Mature embryo.
(K) Endosperm of a globular-stage embryo (the embryo is out of the section plane and cannot be seen).
(L) Heart-stage embryo hybridized with an *ATML1* sense RNA probe as a control.
a, apical cell; b, basal cell; c, cotyledons; cc, central cell; en, endosperm; ep, embryo proper; et, endothelium; fe, fertilized egg; hs, hypophysis; hy, hypocotyl; pd, protoderm; rm, root meristem; s, suspensor; sm, shoot meristem. Bars = 25 μm.

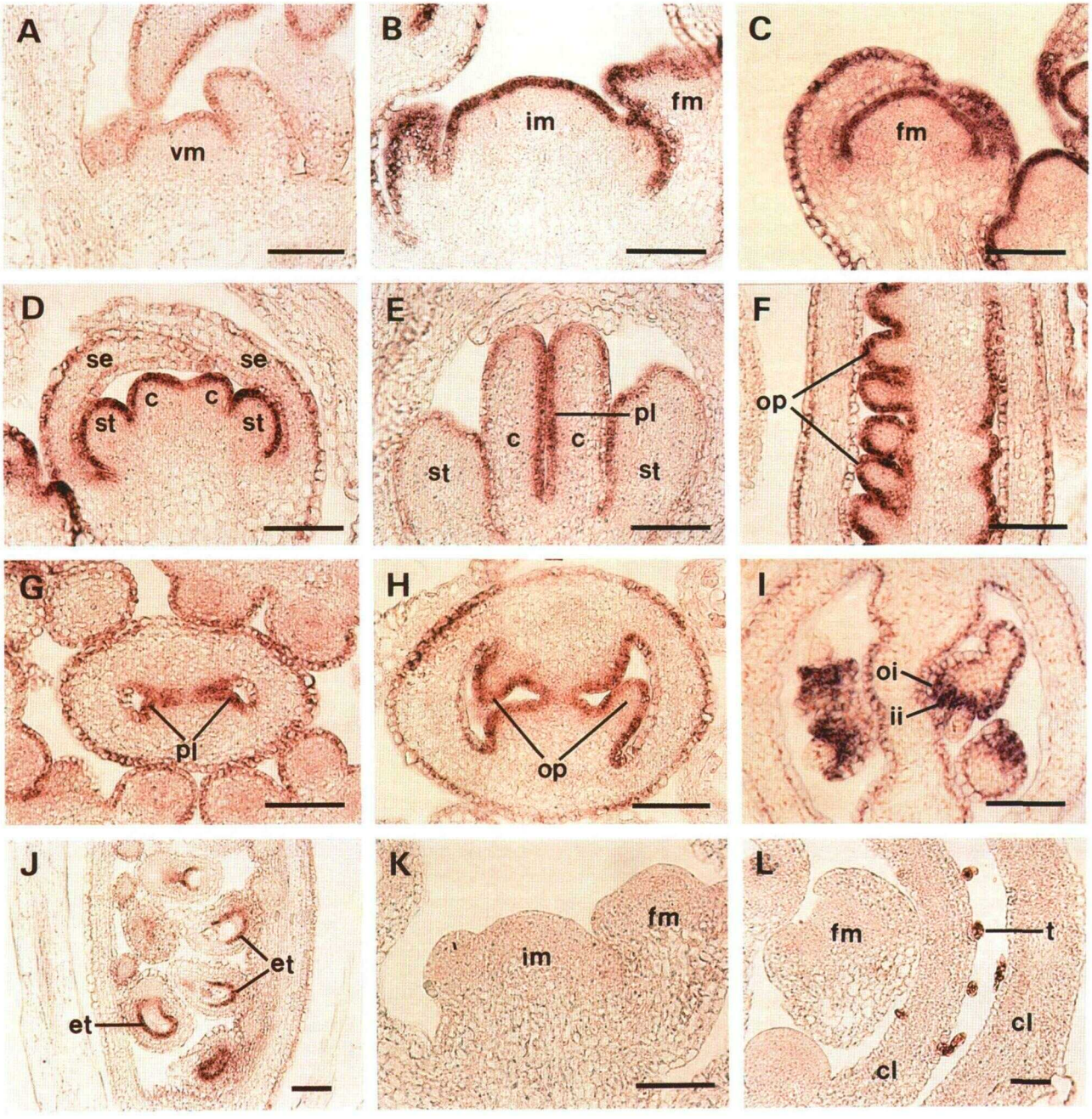

Figure 6. In Situ Localization of *ATML1* mRNA in Shoot Meristems and Developing Floral Organs.

Longitudinal and transverse sections (7 μm thick) through the shoot meristem and flower buds were hybridized with an *ATML1* antisense RNA probe (**[A]** to **[J]**), an *ATML1* sense RNA probe as a control (**K**), or a *GL2* antisense RNA probe (**L**). Probes were labeled with digoxigenin-UTP. The transcript-specific hybridization signal is visualized as purple color. **(A)** to **(F)** and **(J)** to **(L)** are longitudinal sections, and **(G)** to **(I)** are transverse sections.

(A) Vegetative shoot meristem of a 7-day-old seedling.

(B) Inflorescence meristem.

(C) Floral meristem.

(D) Young floral bud.

(E) Developing carpel and placenta.

(F) Ovule primordia.

DISCUSSION

ATML1 Defines a New Class of Homeobox Genes

The *ATML1* cDNA encodes a hypothetical protein that contains a homeodomain DNA binding motif (Figures 1A and 2B). The homeodomain forms three α-helical regions, with helix 2 and helix 3 comprising a helix-turn-helix structure (Gehring et al., 1990, 1994). Within the homeodomain, the recognition helix 3 is responsible for making DNA base contact along the major groove of the DNA, and the N-terminal flexible arm makes additional specific contacts to bases in the adjacent minor groove (Gehring et al., 1990; Wolberger et al., 1991). In the third recognition helix, ATML1 contains all four of the invariant amino acids conserved in all of the homeodomains (Figure 1A; W-49, F-50, N-52, and R-54) (Wolberger et al., 1991; Gehring et al., 1994) and four of six additional amino acids at other conserved positions along the homeodomain (Laughon, 1991). Therefore, it is likely that *ATML1* encodes a true homeobox transcription factor.

In their classification of plant homeodomain proteins, Kerstetter et al. (1994) considered GL2 as a separate plant homeodomain protein not belonging to any particular class. In this study, based on sequence similarity inside and outside of the homeodomain, we show that the Phalaenopsis O39 and Arabidopsis ATML1 homeodomain proteins are additional members of the HD-GL2 class (Figures 1 and 2). All three homeodomains share 60% identity among each other. Especially noteworthy is that all of the three proteins share 13 identical amino acids in the third recognition helix, which suggests that they all recognize the same set of downstream target genes. However, although the third recognition helix is largely responsible for making sequence-specific contact with the DNA, it was shown that other regions of the homeodomain and sequence differences outside of the homeodomain may also be involved in selective protein–protein interactions with other *trans*-acting factors and therefore contribute to functional specificity (reviewed in Kornberg, 1993; Gehring et al., 1994). Therefore, it is reasonable that in spite of the high sequence similarity between the HD-GL2 genes, they may recognize different target DNA sequences.

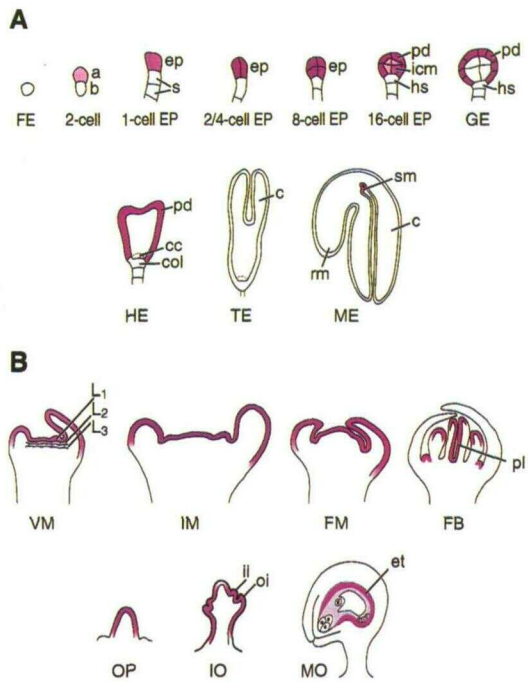

Figure 7. Schematic Representation of *ATML1* mRNA Accumulation during Embryo, Shoot, and Flower Development.

(A) *ATML1* mRNA accumulation (purple color) during embryo development. Morphological features and stages are as follows: a, apical cell; b, basal cell; c, cotyledon; cc, central cell; col, columella; ep, embryo proper; FE, fertilized egg; GE, globular-stage embryo; HE, heart embryo; hs, hypophysis; icm, inner cell mass; ME, mature embryo; pd, protoderm; rm, root meristem; s, suspensor; sm, shoot meristem; TE, torpedo-stage embryo.

(B) *ATML1* mRNA accumulation (purple color) during shoot and flower development. Morphological features and stages are as follows: et, endothelium; FB, flower bud; FM, floral meristem; ii, inner integument; IM, inflorescence meristem; IO, intermediate-stage ovule; MO, mature ovule; oi, outer integument; OP, ovule primordium; pl, placenta; VM, vegetative meristem.

Figure 6. (continued).

(G) Young ovary before ovule initiation.
(H) Ovary with ovule primordia.
(I) Ovules at the intermediate stage of integument initiation.
(J) Flower with mature ovules.
(K) Inflorescence meristem hybridized with an *ATML1* sense RNA probe as a control.
(L) Inflorescence meristem hybridized with a *GL2* antisense RNA probe.
c, carpel; cl, cauline leaf; et, endothelium; fm, floral meristem; ii, inner integument; im, inflorescence meristem; oi, outer integument; op, ovule primordium; pl, placenta; se, sepal; st, stamen; t, trichome; vm, vegetative meristem. Bars = 50 μm.

Surprisingly, apart from O39 and GL2, the ATML1 homeodomain is most similar to the Drosophila engrailed homeodomain homologs (Wray et al., 1995) rather than to other reported plant homeodomains. The *engrailed* locus in Drosophila is a patterning gene that plays an important role in organizing the segmented body plan of the embryo by defining the anterior–posterior boundary of the parasegments (Kornberg et al., 1985).

Interestingly, both *GL2* and *ATML1*, the two Arabidopsis members of the HD-GL2 class, are expressed specifically in the L1 layer of the shoot apical meristem, the protoderm, or the developing epidermis. Although *ATML1* is expressed in the entire L1 layer of the meristem, *GL2* is expressed only in specific epidermal cells that form trichomes (Figure 6L; Rerie et al., 1994). In Phalaenopsis ovules, it was shown that *O39* was first expressed in the placental epidermis and later in the ovule primordium and archesporial cell (Nadeau et al., 1996). By reexamining these observations, we further suggest that in Phalaenopsis, *O39* is expressed specifically in the placental epidermis, the protoderm of ovule primordia, and the outer cell layer surrounding the archesporial cell (Nadeau et al., 1996). Therefore, it seems that *ATML1*, *GL2*, and *O39* share a common L1 layer–specific or dermal-specific pattern of expression. In addition to these members, DNA gel blot analysis suggested that there is probably at least one more Arabidopsis member in this class (Figure 3B). It is reasonable to assume that the HD-GL2 genes became specialized during plant evolution to regulate developmental decisions that establish the dermal layer of the shoot system. Indeed, in the case of other plant homeodomain classes, such as HD-KN1, it was suggested that they share a common pattern of expression and evolutionary function in regulating events within the shoot apical meristem (Jackson et al., 1994; Kerstetter et al., 1994).

The two Arabidopsis members of the HD-GL2 class have been mapped to different chromosomes: whereas *GL2* is located on chromosome 1 (Rerie et al., 1994), *ATML1* mapped to chromosome 4 (Figure 3C). It seems that unlike the *Hox* gene clusters in animals (Gehring et al., 1994), most plant homeobox genes, including those of the HD-GL2 class, are dispersed within the genome. This is similar to what has been observed in maize, in which the 13 members of the *KN1*-like homeobox gene class map to eight of the 10 different chromosomes (Kerstetter et al., 1994).

Apical–Basal Pattern Formation and *ATML1* mRNA Accumulation

In Arabidopsis embryos, apical–basal pattern formation begins with the first asymmetric division of the zygote that produces two unequal daughter cells of distinct developmental fates (Goldberg et al., 1994; Jurgens, 1995). Cell lineage analysis showed that the small apical cell gives rise to most of the embryo proper, whereas the large basal cell forms the root meristem and the suspensor (Mansfield and Briarty, 1991; Dolan et al., 1993; Scheres et al., 1994). Our results show that after the first asymmetric division of the zygote, *ATML1* mRNA gradually appeared in the apical cell but not in the basal cell (Figures 5A to 5D). Moreover, during embryo development, *ATML1* mRNA continued to accumulate specifically in the regions that were formed from the apical cell but not in the suspensor, hypophysis, central cell, and columella that were formed from the basal cell (Figures 5B to 5G).

These data provide the earliest molecular marker for the definition of apical–basal pattern formation in plants. This is a developmental period in embryogenesis for which there are no early molecular or cellular markers (Thomas, 1993; Goldberg et al., 1994). Furthermore, the fact that *ATML1* encodes a homeodomain protein suggests that it may participate in the regulatory network of transcription factors whose interactions are required for specifying embryo development (Goldberg et al., 1994).

Clues to the nature of the factors that regulate *ATML1* expression in the apical cell may come from research in animal systems in which early axis pattern formation after the first asymmetric division of the zygote is regulated by maternal determinants, whether localized outside in the maternal tissue or inside in the cytoplasm of the egg (Gurdon, 1992; St Johnston and Nusslein-Volhard, 1992). It is possible that the differential accumulation of *ATML1* mRNA in the apical cell was predetermined during the establishment of polarity in the zygote that later leads to the formation of a densely cytoplasmic apical cell (Mansfield and Briarty, 1991). The asymmetric division step is perhaps also associated with the accumulation of high levels of the factor(s) that regulates the expression of *ATML1*. Alternatively, it could be the position of the apical cell after the asymmetric division relative to other signals produced by surrounding maternal tissues that determines *ATML1* expression.

Radial Pattern Formation and *ATML1* mRNA Accumulation

Radial pattern formation first begins with the differentiation of the protoderm, which is the first defined embryonic tissue (Mansfield and Briarty, 1991; Goldberg et al., 1994; Jurgens, 1995). We found that after the eight cells of the octant proembryo have divided periclinally to form the outer layer or the protoderm, *ATML1* mRNA gradually declined in the inner cell mass and its expression became restricted specifically to the protoderm (Figure 5F). The fact that *ATML1* became restricted to the protoderm from the beginning of its formation suggests its possible involvement in the specification of this layer. Our observations about the early layer-specific accumulation of *ATML1* mRNA in the protoderm are in agreement with other histological studies and those reported earlier for Arabidopsis *raspberry* embryos, suggesting that radial pattern formation and differentiation of the three tissue layers have already occurred by the globular stage of embryogenesis (Mansfield and Briarty, 1991; Yadegari et al., 1994).

In previous studies concerning the differentiation of the embryonic cell layers, the *Arabidopsis* lipid transfer protein (*AtLPT1*) mRNA was used as a molecular marker for detec-

tion of the epidermal layer (Sterk et al., 1991; Thoma et al., 1994). However, in Arabidopsis embryos, *AtLPT1* mRNA could not be detected in the early globular, heart, or even torpedo stages of embryo development but only in the later bent cotyledon and mature embryo stages (Yadegari et al., 1994). In this study, we demonstrate that *ATML1* mRNA accumulates specifically in the protoderm at the dermatogen or 16-cell embryo stage and therefore may provide a useful molecular marker for studying the earliest stages of radial pattern formation during embryogenesis (Figures 5F to 5H).

During animal development, the three primary germ layers of the embryo are formed during gastrulation by directed cell migration (Beddington and Smith, 1993; Kessler and Melton, 1994). Plants, however, lack cell movement and instead have different planes of cell divisions. Because *ATML1* was expressed uniformly in all cells of the octant-stage proembryo, becoming restricted to the protoderm only after the periclinal divisions of these cells (Figure 5F), it is possible that these cell divisions are directly involved in regulating *ATML1* expression. Moreover, because the protoderm cells only divide in an anticlinal plane, it is possible that the anticlinal cell divisions are involved in the maintenance of *ATML1* expression in this layer.

Another possibility for the control of *ATML1* expression in the protoderm is the existence of specific regulatory signals (Gurdon, 1992; Beddington and Smith, 1993; Kessler and Melton, 1994). These signals could be a morphogen that generates radial patterns from a signaling center, as described for *Caenorhabditis elegans* (Kenyon, 1995), or other positive or negative regulator signals. In the mouse, for example, the homeobox patterning gene *Otx2* was restricted to the ectoderm layer by positive and negative signals from the more inner mesoderm layer (Ang et al., 1994).

In addition to the embryo, *ATML1* mRNA was also detected in the developing endosperm (Figure 5K). This observation is in agreement with studies that were done in maize and barley, which suggest that a large set of seed-specific genes are expressed in both the endosperm and the embryo (reviewed in Lopes and Larkins, 1993). The shared accumulation of *ATML1* mRNA in the embryo and endosperm also supports the hypothesis that the endosperm evolved from a supernumerary embryo, thus having a common evolutionary embryonic origin (Friedman, 1990).

Shoot Meristem and Flower Development and *ATML1* mRNA Accumulation

In the mature embryo, *ATML1* mRNA became restricted to the protoderm of the shoot apical meristem (Figure 5J). Other homeobox genes that are known to be involved in meristem formation are *KN1* in maize and *STM* in Arabidopsis. In contrast to *ATML1* that was expressed from the first asymmetric division of the zygote, both *KN1* and *STM* are expressed only after the first histological recognition of the shoot meristem at the heart–torpedo embryo stages (Smith et al., 1995; Long et al., 1996). In the Arabidopsis shoot meristem, *ATML1* is expressed only in the L1 layer, whereas *STM* is expressed in the complete meristem dome. Therefore, it is possible that there are some interactions between the genes in controlling meristem formation and function.

After germination, the meristem L1 layer–specific pattern of *ATML1* gene expression was maintained in the vegetative shoot apical meristem, inflorescence and floral meristems, and young floral organ primordia (Figures 6A to 6D). In all cases, *ATML1* mRNA accumulated only in the undifferentiated actively dividing protoderm cells and not in the mature epidermal cells (Figures 6A to 6D). Other genes that were also found to be highly expressed in the L1 layer of the shoot apical meristems are those in carrot, tobacco, and Arabidopsis that encode lipid transfer proteins (Sterk et al., 1991; Fleming et al., 1992; Thoma et al., 1994), tomato polyphenoloxidase (Shahar et al., 1992), and several unknown Pachyphytum sequences (Clark et al., 1992). However, besides *ATML1*, all of the genes mentioned above are also expressed in the epidermis of mature organs, such as leaves and stems, and were suggested to be involved in determining the specific function of the epidermis (Clark et al., 1992; Thoma et al., 1994). As a meristem L1 layer–specific homeobox gene, *ATML1* may be involved in the transcriptional regulation of these other downstream target genes.

During flower development, *ATML1* mRNA gradually declined in the protoderm of most floral organs and became restricted to the placenta of the ovary and later to the ovule primordium and integuments (Figures 6D to 6H). In the mature ovule, *ATML1* mRNA accumulated in the endothelium surrounding the embryo sac (Figure 6J). The continuous expression of *ATML1* in the protoderm of ovules and integuments indicates that the ovule retains some meristematic properties, thereby supporting the theory about the possible phylogenic origin of the ovule from the shoot (Herr, 1995). Because the ovule is the last organ determined from the shoot meristem, our data show that *ATML1* is expressed throughout the complete diploid life cycle of the plant, from the first division of the diploid zygote (Figure 5B) to production of the endothelium layer surrounding the haploid embryo sac (Figure 6J).

METHODS

Plant Material

Seeds of *Arabidopsis thaliana* ecotype Landsberg *erecta* were sown in Sunshine mix No. 1 (Sun Gro Horticulture Inc., Bellevue, WA) and grown in a growth chamber at 22 to 25°C under continuous fluorescence light.

Library Screening

A floral bud cDNA library (ABRC; Weigel et al., 1992) was screened by plaque hybridization with the Phalaenopsis *O39* homeobox cDNA as a probe (Nadeau et al., 1996), following standard procedures (Sambrook et al., 1989). Hybridization was performed under stringent conditions with a probe labeled to high specific activity by random priming (Boehringer Mannheim) with ^{32}P-dCTP.

Sequence Analysis

Sequencing was performed by the dideoxynucleotide chain termination method (Sanger et al., 1977), using Sequenase Version 2 (U.S. Biochemical/Amersham). Sequence-specific primers were synthesized and used to generate overlapping sequence information. Sequence analysis and multiple sequence alignment (PILEUP) were accomplished by using the Genetics Computer Group (Madison, WI) and BLAST (Altschul et al., 1990) computer programs. The GenBank accession number of *ATML1* is U37589.

Mapping

The chromosomal location of *ATML1* on the recombinant inbred (RI) map was determining by segregation analysis of a restriction fragment length polymorphism among 100 RI lines, using an *ATML1* gene-specific probe (Figure 3A, probe 2) as described by Lister and Dean (1993). The location of *ATML1* on the classical genetic map was estimated by multiplying its location on chromosome 4 of the RI map by (total length of classical chromosome)/(total length of RI chromosome).

DNA Gel Blot Analysis

DNA was extracted from leaf tissue by using the procedure described by Jofuku and Goldberg (1988). Ten micrograms of genomic DNA was digested with EcoRI, BamHI, or HindIII (Promega), separated on an 0.8% agarose gel, and blotted onto a Nytran membrane (Schleicher & Schüll). Blots were hybridized with a probe labeled to high specific activity by random priming (Boehringer Mannheim) with ^{32}P-dCTP at 37°C in 50% formamide, 5 × SSC (1 × SSC is 0.15 M NaCl, 0.015 M sodium citrate), 0.05 M phosphate buffer, pH 7, 5 × Denhardt's solution (1 × Denhardt's is 0.02% Ficoll, 0.02% PVP, 0.02% BSA), 0.2 mg/mL sheared denatured salmon testes DNA (Type III; Sigma), and 0.2% SDS. For low-stringency conditions, blots were washed twice at 37°C for 20 min with 2.0 × SSC and 0.1% SDS. For high-stringency conditions, blots were washed three times for 20 min at 55, 60, and 63°C with 0.2 × SSC and 0.1% SDS. Autoradiography was performed at −80°C using Kodak XAR-5 film and one intensifying screen (Cornex Lightning Plus; Du Pont). Blots were exposed for 2 to 3 days.

RNA Gel Blot Analysis

The methods for RNA extraction as well as RNA gel blot hybridization have been described previously (O'Neill et al., 1993). Poly(A)$^+$ RNA was isolated using paramagnetic oligo(dT) beads (Dynabeads; Dynal, Lake Success, NY), according to manufacturer's suggestions. Poly(A)$^+$ RNA (1 μg per lane) was separated on an 0.8% formaldehyde agarose gel and blotted onto a Nytran membrane. Blots were hybridized with a probe labeled to high specific activity by random priming (Boehringer Mannheim) with ^{32}P-dCTP at 42°C, as described for DNA blot hybridization (see above). Blots were washed three times for 20 min at 55, 60, and 63°C with 0.2 × SSC, 0.1% SDS solution and autoradiographed at −80°C using Kodak XAR-5 film and an intensifying screen (Cornex Lightning Plus; Du Pont). Blots were exposed for 2 to 5 days.

In Situ Hybridization

Tissues from different stages of shoots, flowers, and siliques were fixed for 4 to 6 hr in 50 mM phosphate buffer, pH 7, 4% paraformaldehyde (Sigma), and 0.1% glutaraldehyde (Polysciences, Warrington, PA). Afterward, the tissues were rinsed in phosphate buffer alone and dehydrated through a graded series of ethanol (10 to 100% [v/v]). The tissues were embedded in Paraplast Plus (Oxford Labware, St. Louis, MO), cut into 7-μm sections, and mounted on Superfrost Plus microscope slides (Fisher Scientific, Pittsburgh, PA). For the synthesis of *ATML1* antisense and sense transcripts, a 1230-bp XbaI-Bsp106I cDNA fragment that does not contain the homeodomain (Figure 3A, probe 2) was ligated into pBluescript II SK− (Stratagene) and transcribed in vitro with digoxigenin-UTP by using T3 or T7 polymerase (Boehringer Mannheim). The *GLABRA2* (*GL2*)-specific RNA probe was synthesized according to Rerie et al. (1994). Prehybridization, hybridization, washings, RNaase treatment, and immunological detection of the incorporated digoxigenin-UTP were performed using a digoxigenin nucleic acid detection system (Boehringer Mannheim), according to the manufacturer's protocol. Photographic images were recorded on Kodak Royal Gold 25 film, using an Olympus BX60 photomicroscope system (Olympus Optical Co., Tokyo, Japan).

ACKNOWLEDGMENTS

We thank Dr. David M. Marks (University of Minnesota, St. Paul) for the *GL2* cDNA. We acknowledge the Arabidopsis Biological Resource Center for the floral bud cDNA library and the Nottingham Arabidopsis Stock Centre and Dr. Clare Lister for the recombinant inbred lines. We also thank Elena Lee for technical assistance. R.P. was supported by a U.S.-Israel Binational Agricultural Research and Development Postdoctoral Fellowship (Award No. FI-0210-95). This research was supported by a grant from the U.S. Department of Agriculture, National Research Initiative Cooperative Grant Program, Plant Growth and Development Program (No. 95-37304-2322) to S.D.O.

Received August 8, 1996; accepted September 25, 1996.

REFERENCES

Altschul, S.F., Gish, W., Miller, W., Myers, E.W., and Lipman, D.J. (1990). Basic local alignment search tool. J. Mol. Biol. **215,** 403–410.

Ang, S., Conlon, R.A., Jin, O., and Rossant, J. (1994). Positive and negative signals from mesoderm regulate the expression of mouse *Otx2* in ectoderm explants. Development **120,** 2979–2989.

Barton, M.K., and Poethig, R.S. (1993). Formation of the shoot apical meristem in *Arabidopsis thaliana*: An analysis of development in the wild type and in the *shoot meristemless* mutant. Development **119,** 823–831.

Beddington, R.S.P., and Smith, J.C. (1993). Control of vertebrate gastrulation: Inducing signals and responding genes. Curr. Opin. Genet. Dev. **3,** 655–661.

Bellmann, R., and Werr, W. (1992). Zmhox1a, the product of a novel maize homeobox gene, interacts with the *Shrunken* 26 bp *feedback* control element. EMBO J. **11,** 3367–3374.

Blum, M., Gaunt, S.J., Cho, K.W.Y., Steinbeisser, H., Blumberg, B., Bittner, D., and De Robertis, E.M. (1992). Gastrulation in the mouse: The role of the homeobox gene *goosecoid.* Cell **69,** 1097–1106.

Boncinelli, E., and Mallamaci, A. (1995). Homeobox genes in vertebrate gastrulation. Curr. Opin. Genet. Dev. **5,** 619–627.

Clark, A.M., Verbeke, J.A., and Bohnert, H.J. (1992). Epidermis-specific gene expression in Pachyphytum. Plant Cell **4,** 1189–1198.

Dolan, L., Janmaat, K., Willemsen, V., Linstead, P., Poethig, S., and Roberts, K. (1993). Cellular organization of the *Arabidopsis thaliana* root. Development **119,** 71–84.

Fleming, A.J., Mandel, T., Hofmann, S., Sterk, P., De Vries, S.C., and Kuhlemeier, C. (1992). Expression pattern of a tobacco lipid transfer protein gene within the shoot apex. Plant J. **2,** 855–862.

Friedman, W.E. (1990). Double fertilization in *Ephedra*, a non-flowering plant: Its bearing on the origin of angiosperms. Science **247,** 951–954.

Gehring, W.J., Muller, M., Affolter, M., Percival-Smith, A., Billeter, M., Qian, Y.Q., Otting, G., and Wuthrich, K. (1990). The structure of the homeodomain and its functional implications. Trends Genet. **6,** 323–329.

Gehring, W.J., Affolter, M., and Burglin, T. (1994). Homeodomain proteins. Annu. Rev. Biochem. **63,** 487–526.

Goldberg, R.B., Paiva, G.D., and Yadegari, R. (1994). Plant embryogenesis: Zygote to seed. Science **266,** 605–614.

Gurdon, J.B. (1992). The generation of diversity and pattern in animal development. Cell **68,** 185–199.

Herr, J.M. (1995). The origin of the ovule. Am. J. Bot. **82,** 547–564.

Jackson, D., Veit, B., and Hake, S. (1994). Expression of the maize *KNOTTED-1* related homeobox genes in the shoot apical meristem predicts patterns of morphogenesis in the vegetative shoot. Development **120,** 405–413.

Jofuku, K.D., and Goldberg, R.B. (1988). Analysis of plant gene structure. In Plant Molecular Biology: A Practical Approach, C.H. Shaw, ed (Oxford, UK: IRL Press Limited), pp. 37–66.

Jurgens, G. (1995). Axis formation in plant embryogenesis: Cues and clues. Cell **81,** 467–470.

Jurgens, G., Torres Ruiz, R.A., and Berleth, T. (1994). Embryonic pattern formation in flowering plants. Annu. Rev. Genet. **28,** 351–371.

Kenyon, C. (1995). A perfect vulva every time: Gradients and signaling cascades in C. elegans. Cell **82,** 171–174.

Kerstetter, R., Volbrecht, E., Lowe, B., Veit, B., Yamaguchi, J., and Hake, S. (1994). Sequence analysis and expression patterns divide the maize *knotted1*-like homeobox genes into two classes. Plant Cell **6,** 1877–1887.

Kessler, D.S., and Melton, D.A. (1994). Vertebrate embryonic induction: Mesodermal and neural patterning. Science **266,** 596–604.

Korfhage, U., Trezzini, G.F., Meier, I., Hahlbrock, K., and Somssich, I.E. (1994). Plant homeodomain protein involved in transcriptional regulation of a pathogen defense-related gene. Plant Cell **6,** 695–708.

Kornberg, T., Siden, I., O'Farrell, P., and Simon, M. (1985). The *engrailed* locus in Drosophila: In situ localization of transcripts reveals compartment-specific expression. Cell **40,** 45–53.

Kornberg, T.B. (1993). Understanding the homeodomain. J. Biol. Chem. **268,** 26813–26816.

Laughon, A. (1991). DNA binding specificity of homeodomains. Biochemistry **30,** 11357–11367.

Lawrence, P.A., and Morata, G. (1994). Homeobox genes: Their function in Drosophila segmentation and pattern formation. Cell **78,** 181–189.

Lincoln, C., Long, J., Yamaguchi, J., Serikawa, K., and Hake, S. (1994). A *knotted1*-like homeobox gene in Arabidopsis is expressed in the vegetative meristem and dramatically alters leaf morphology when overexpressed in transgenic plants. Plant Cell **6,** 1859–1876.

Lister, C., and Dean, C. (1993). Recombinant inbred lines for mapping RFLP and phenotypic markers in *Arabidopsis thaliana*. Plant J. **4,** 745–750.

Long, J.A., Moan, E.I., Medford, J.I., and Barton, M.K. (1996). A member of the KNOTTED class of homeodomain proteins encoded by the *STM* gene of *Arabidopsis*. Nature **379,** 66–69.

Lopes, M.A., and Larkins, B.A. (1993). Endosperm origin, development, and function. Plant Cell **5,** 1383–1399.

Ma, H., McMullen, M.D., and Finer, J.J. (1994). Identification of a homeobox-containing gene with enhanced expression during soybean (*Glycine max* L.) somatic embryo development. Plant Mol. Biol. **24,** 465–473.

Mansfield, S.G., and Briarty, L.G. (1991). Early embryogenesis in *Arabidopsis thaliana*. II. The developing embryo. Can. J. Bot. **69,** 461–476.

Mattsson, J., Soderman, E., Svenson, M., Borkird, C., and Engstrom, P. (1992). A new homeobox–leucine zipper gene from *Arabidopsis thaliana*. Plant Mol. Biol. **18,** 1019–1022.

Meinke, D.W. (1995). Molecular genetics of plant embryogenesis. Annu. Rev. Plant Physiol. Plant Mol. Biol. **46,** 369–394.

Nadeau, J.A., Zhang, X.S., Li, J., and O'Neill, S.D. (1996). Ovule development: Identification of stage-specific and tissue-specific cDNAs. Plant Cell **8,** 213–239.

O'Neill, S., Nadeau, J.A., Zhang, X.S., Bui, A.Q., and Halevy, A.H. (1993). Interorgan regulation of ethylene biosynthetic genes by pollination. Plant Cell **5,** 419–432.

Quaedvlieg, N., Dockx, J., Rook, F., Weisbeek, P., and Smeekens, S. (1995). The homeobox gene *ATH1* of Arabidopsis is derepressed in the photomorphogenetic mutants *cop1* and *det1*. Plant Cell **7,** 117–129.

Reiser, L., Modrusan, Z., Margossian, L., Samach, A., Ohad, N., Haughn, G.W., and Fischer, R.L. (1995). The *BELL1* gene encodes a homeodomain protein involved in pattern formation in the Arabidopsis ovule primordium. Cell **83,** 735–742.

Rerie, W.G., Feldmann, K.A., and Marks, M.D. (1994). The *GLABRA2* gene encodes a homeodomain protein required for normal trichome development in *Arabidopsis*. Genes Dev. **8,** 1388–1399.

Ruberti, I., Sessa, G., Lucchetti, S., and Morelli, G. (1991). A novel class of plant proteins containing a homeodomain with a closely linked leucine zipper motif. EMBO J. **10,** 1787–1791.

Sambrook, J., Fritsch, E.F., and Maniatis, T. (1989). Molecular Cloning: A Laboratory Manual, 2nd ed. (Cold Spring Harbor, NY: Cold Spring Harbor Laboratory).

Sanger, F., Nicklen, S., and Coulson, A.R. (1977). DNA sequencing with chain terminating inhibitors. Proc. Natl. Acad. Sci. USA **74,** 5463–5467.

Satina, S., Blakeslee, A.F., and Avery, A.G. (1940). Demonstration of the three germ layers in the shoot apex of *Datura* by means of induced polyploidy in periclinal chimeras. Am. J. Bot. **27,** 895–905.

Schena, M., and Davis, R.W. (1992). HD-Zip proteins: Members of an *Arabidopsis* homeodomain superfamily. Proc. Natl. Acad. Sci. USA **89,** 3894–3898.

Schena, M., and Davis, R.W. (1994). Structure of homeobox–leucine zipper genes suggests a model for the evolution of gene families. Proc. Natl. Acad. Sci. USA **91,** 8393–8397.

Scheres, B., Wolkenfelt, H., Willemsen, V., Terlouw, M., Lawson, E., Dean, C., and Weisbeek, P. (1994). Embryonic origin of the

Arabidopsis primary root and root meristem initials. Development **120,** 2475–2487.

Schindler, U., Beckmann, H., and Cashmore, A.R. (1993). HAT3.1, a novel *Arabidopsis* homeodomain protein containing a conserved cysteine-rich region. Plant J. **4,** 137–150.

Schmidt, A. (1924). Histologische Studien an phanerogamen Vegetationspunkten. Bot. Arch. **8,** 345–404.

Shahar, T., Hennig, N., Gutfinger, T., Hareven, D., and Liftschitz, E. (1992). The tomato 66.3-kD polyphenoloxidase gene: Molecular identification and developmental expression. Plant Cell **4,** 135–147.

Shawlot, W., and Behringer, R.R. (1995). Requirement for *Lim1* in head-organizer function. Nature **374,** 425–430.

Sinha, N.R., Williams, R., and Hake, S. (1993). Overexpression of the maize homeobox gene, *KNOTTED1*, causes a switch from determinate to indeterminate cell fates. Genes Dev. **7,** 787–795.

Smith, L.G., Jackson, D., and Hake, S. (1995). Expression of *Knotted1* marks shoot meristem formation during maize embryogenesis. Dev. Genet. **16,** 344–348.

Sterk, P., Booij, H., Schellekens, G.A., Van Kammen, A., and De Vries, S.C. (1991). Cell-specific expression of the carrot EP2 lipid transfer protein gene. Plant Cell **3,** 907–921.

St Johnston, D., and Nusslein-Volhard, C. (1992). The origin of pattern and polarity in Drosophila embryo. Cell **68,** 201–219.

Sussex, I.M. (1989). Developmental programming of the shoot meristem. Cell **56,** 225–229.

Thoma, S., Hecht, U., Kippers, A., Botella, J., De Vries, S., and Somerville, C. (1994). Tissue-specific expression of a gene encoding a cell wall–localized lipid transfer protein from Arabidopsis. Plant Physiol. **105,** 35–45.

Thomas, T.L. (1993). Gene expression during plant embryogenesis and germination: An overview. Plant Cell **5,** 1401–1410.

Volbrecht, E., Veit, B., Sinha, N., and Hake, S. (1991). The developmental gene *Knotted1* is a member of a maize homeobox gene family. Nature **350,** 241–243.

Weigel, D., Alvarez, J., Smyth, D.R., Yanofsky, M.F., and Meyerowitz, E.M. (1992). LEAFY controls floral meristem identity in Arabidopsis. Cell **69,** 843–859.

West, M.A.L., and Harada, J.J. (1993). Embryogenesis in higher plants: An overview. Plant Cell **5,** 1361–1369.

Wolberger, C., Vershon, A.K., Liu, B., Johnson, A.D., and Pabo, C.O. (1991). Crystal structure of a MATα2 homeodomain-operator complex suggests a general model for homeodomain–DNA interactions. Cell **67,** 517–528.

Wray, C.G., Jacobs, D.K., Kostriken, R., Vogler, A.P., Baker, R., and De Salle, R. (1995). Homologues of the engrailed gene from five molluscan classes. FEBS Lett. **365,** 71–74.

Yadegari, R., de Paiva, G.R., Laux, T., Koltunow, A.M., Apuya, N., Zimmerman, J.L., Fischer, R.L., Harada, J.J., and Goldberg, R.B. (1994). Cell differentiation and morphogenesis are uncoupled in Arabidopsis *raspberry* embryos. Plant Cell **6,** 1713–1729.